LHCb note 2009-034

The Hadron Alley of the LHCb High Level Trigger

Jose Angel Hernando
CERN, Switzerland
on leave from: *Universidade de Santiago de Compostela, Spain*

Diego Martinez, Xabier Cid
Universidade de Santiago de Compostela, Spain

Gabriel Guerrer, Alvaro Gomes
Centro Brasileiro de Pesquisas Fisicas (CBPF), Rio de Janeiro, Brazil

Johannes Albrecht
Physikalisches Institut, Heidelberg, Germany

Abstract

This note describes the "hadron alley", the list of algorithms that selects B meson decays into hadrons in the first level of the LHCb software trigger (HLT1). The alley aims to obtain a rate reduction of at least a factor 30 with respect to the input rate of the hardware trigger (L0), while keeping the efficiency on offline selected B decays into hadrons as high as possible. The hadron alley implements the "L0 confirmation" strategy, that requires that HLT1 trigger decisions are based on particles that triggered the L0. The performance of the alley is presented and some alternative configurations of the L0 hadron trigger and the hadron alley are discussed.

Contents

1 Introduction

The LHCb experiment will study CP violation and rare decays in the B and D mesons produced at the LHC. These studies require the selection of B decays into specific final states. For this reason, the LHCb trigger has been designed to be highly flexible and capable of triggering on hadrons, muons, electrons and photons. Some of the B decays that are relevant for the physics analysis have only hadrons in the final state, such as $B^0 \to h^+h^-$, $B^0_s \to D^\pm_s K^\mp$ or $B^\pm \to D(K^\pm\pi^\mp)K^\pm$. This note describes the list of algorithms, known as "hadron alley", that selects B decays into hadrons in an inclusive way in the first software level (HLT1).

The trigger of LHCb is divided in two levels: Level 0 (L0) and High Level Trigger (HLT) [1]. The L0 is a hardware trigger that reduces the rate from the 10 MHz of visible interactions (at the nominal luminosity of 2×10^{32} cm^{-2}s^{-1}) to 1 MHz. It uses the information from the calorimeters, the pile-up system and the muon detector. The L0 trigger is divided in "lines": muon, hadron, photon, etc. The L0 muon line requires the presence of a muon of "high" transverse momentum (P_T >1.3 GeV), and the hadron trigger, a large transverse energy hadron cluster in the calorimeters (E_T >3.5 GeV). In addition, the L0 trigger has the capability of vetoing high multiplicity or multi-primary vertices events to stop further processing of complex events. The full detector data is then readout at 1 MHz. Events passing the L0 are filtered in a dedicated farm, called Event Filter Farm (EFF), where the HLT application is executed, producing an output rate of 2 kHz. At this rate, events are stored on disk for further processing. The size and computational power of the EFF determine the algorithms that can be run in the HLT. Ideally, one would like to run the offline reconstruction and selection of the B decays, but this is far from the current capabilities of the EFF.

The HLT is itself divided in two levels, called HLT1 and HLT2. HLT1 aims for a large rate reduction (∼3%) by performing a partial reconstruction of the event. Depending on the the L0 trigger type, the HLT1 executes different sets of algorithms, called "alleys". This note describes the hadron alley, other alleys as the muon or muon + track are described in Refs. [2] and [3]. In the alleys, the L0 objects are used as starting point of the reconstruction: they define a region of interest where the data is decoded. This reduces the CPU consumption time of the decoding and the pattern recognition algorithms. At the output rate of the HLT1 (∼30 kHz) the HLT2 algorithms perform the full reconstruction of the event (as similar as possible to the offline reconstruction) and apply several inclusive selections of B decays.

The first part of the hadron alley is called "L0 confirmation", where a track is reconstructed starting from a L0 hadron cluster that fired the L0 hadron line. This track is called "L0 confirmed track". The alley is divided into two independent sequences of algorithms or "lines", called "single hadron" and "dihadron". The first one sets a trigger decision based only on the L0 confirmed track, while in the second one, the decision is taken on a secondary vertex made with the L0 confirmed track and an extra track, called "companion track".

To understand the performance of the trigger on the selected B signals it is useful to classify the events into the categories called "TIS" and "TOS" [4] [5]. An event is Trigger On Signal (TOS) if the B daughters are responsible of the trigger; events in which other particles but the B daughters triggered the event, are classified as Trigger Independent of the Signal (TIS). Note that these categories are not exclusive. The effect of the trigger cuts on the selected B decays can be understood using TOS events. Along the note most of the signal efficiencies are given for TOS events.

In the following sections the L0 hadron, L0 confirmation and the single and dihadron lines are described. In the last section, different configurations of the L0 and hadron alley are presented.

The results of this note were obtained using the DaVinci application version v22r0p2, with 10^5 L0 filtered mb events, and 1k of offline selected $B^0 \to h^+h^-$, $B^0_s \to D^\pm_s h^\mp$, $B^0_s \to \Phi\Phi$ and $B^0 \to D^0 K^{*0}$ events. The data used correspond to the Monte Carlo simulation configuration called "DC06". The efficiencies for the signal are computed with respect to offline selected events and the timing is taken from the output of the DaVinci application on a lxplus machine 2.7×2.8 GHz Xeon CPU. This machine is approximately 30% faster than a core of the EFF.

2 L0 hadron trigger

At L0, there are a list of global quantities that can be used to veto multi-primary vertices events. These quantities are: the multiplicity of the SPD detector, the Pile Up information on the number of tracks in a second primary vertex and the hit multiplicity in the Pile Up System [6]. The cuts on these quantities (table 1) are called Global Event Cuts (GEC). The GEC reduce the average num-

Quantity	Value
Tracks in 2nd vertex	<3
Pile-Up multiplicity	<112 hits
SPD multiplicity	<280 hits
Total E_{T}	>5 GeV

Table 1: List of the Global Event Cuts.

	L0	L0 TOS
$B^0 \to h^+h^-$	50	38
$B^0_s \to \Phi\Phi$	34	19
$B^0_s \to D^{\pm}_s h^{\mp}$	44	29
$B^0 \to D^0 K^{*0}$	32	23

Table 2: L0 and L0 TOS efficiency (in %) for some B decays.

ber of primary vertices from 1.4 (at the nominal luminosity 2×10^{32} cm^{-2} s^{-1}) to 1.1.

The L0 calorimeter clusters are constructed by adding the deposited energy on the 2×2 adjacent cells in the hadronic calorimeter (HCal) and the energy deposited in the cells of the electromagnetic calorimeter (ECal) in front. For each of the candidates the total transverse energy (E_{T}) is computed. An event passes the L0 hadron trigger if there is a L0 hadron cluster with E_{T} >3.5 GeV and it is not vetoed by the GEC. The L0 hadron trigger is described with detail in Ref. [6]. Figure 1 shows the rate vs the E_{T} threshold of the L0 hadron clusters. The maximum rate allowed at the L0 is 1 MHz, therefore the minimum cut is E_{T} >3 GeV. The rate of the L0 hadron channel, with a cut in E_{T} >3.5 GeV, is 600 kHz. Figure 2 shows the L0 TOS efficiency for some channels as a function of the E_{T} threshold. Table 2 shows the L0 and L0 TOS efficiencies for some channels. Note that the L0 efficiency is below 50% and the L0 TOS efficiency is lower, with 25%-45% of the events, depending on the B decays, where the L0 hadron channel was not triggered by the B daughters.

3 L0 hadron confirmation

The L0 confirmation part of the hadron alley is common to the single and dihadron lines. If there is a L0 candidate, that is, a L0 hadron cluster that fired the L0 trigger, then the L0 confirmation part checks that exists a track associated to that L0 candidate. Figure 3 shows the average number of L0 candidates above a E_{T} threshold. Note that the

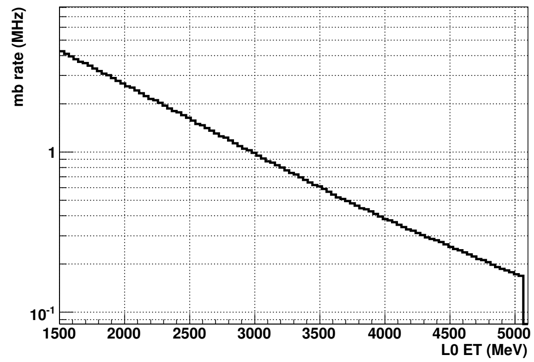

Figure 1: Rate vs E_{T} threshold for events that passed the GEC.

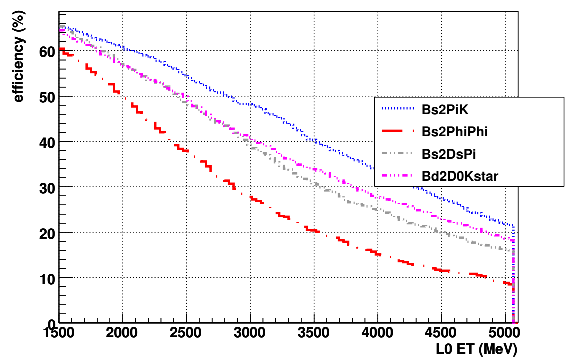

Figure 2: L0 TOS efficiency vs E_{T} threshold for events that passed the GEC.

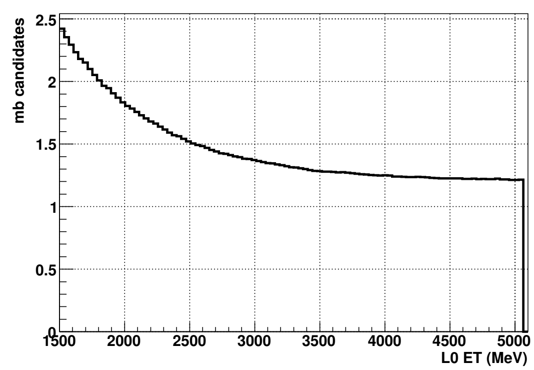

Figure 3: Number of L0 candidates above a given E_{T} threshold for events that passed the GEC.

number of candidates is only 1.3 for $E_{\mathrm{T}} > 3.5$ GeV and it is quite constant in the rage between 3 and 5 GeV. As there are few L0 candidates per event, there are few tracks to be reconstructed.

There are two possibilities of doing the L0 con-

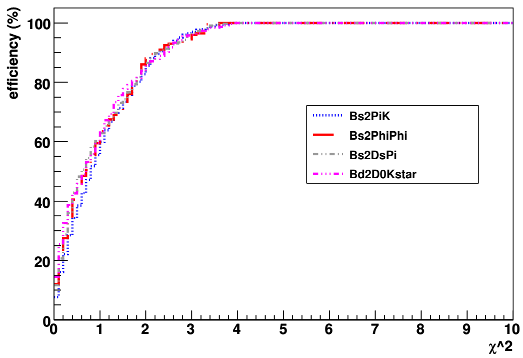

Figure 4: Efficiency vs $\chi^2(rz)$ cut.

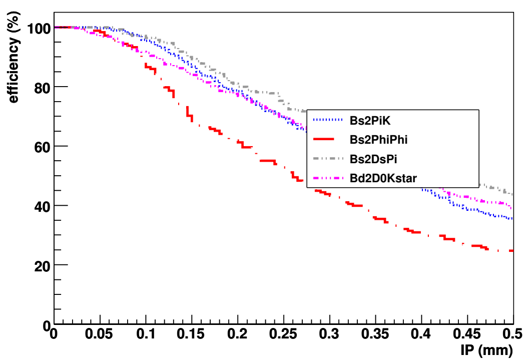

Figure 5: Efficiency vs the IP cut on the L0 confirmed track.

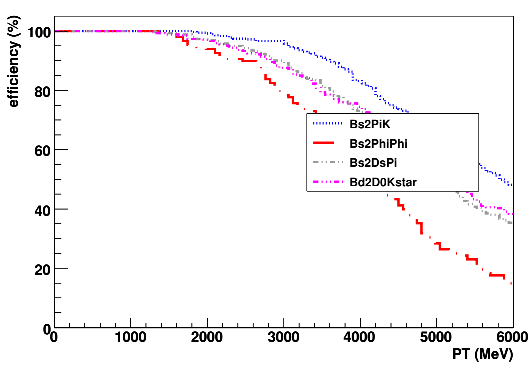

Figure 6: Efficiency vs the P_{T} cut on the L0 confirmed track.

firmation, starting the search of the tracks in the Velo or the tracking stations (Ref. [7] [8]). In this note, the first one is described.

Thanks to the Velo design in r and ϕ sensors, it is possible to reconstruct first the tracks in the (r, z) plane. The pattern recognition algorithm searches for tracks originated along the beam line, this reduces the number of initial valid combinations of hits used as seeds to search for tracks. These tracks are then used to reconstruct the primary vertices [9] of the pp interactions.

After that, the (r, z) Velo tracks that match with a L0 candidate are selected. In first approximation, the effect of the magnet can be consider as a change in the slope of the track depending on the modulus of its momentum. The matching method is based on a χ^2 quantity computed from the difference of the slope of the (r, z) Velo track and the slope computed from the cluster position and the origin of the LHCb system, where the cluster position is corrected by the expected deviation in the (x, y) plane of the calorimeter according with the cluster energy. The details of this method are described in Ref. [10]. Figure 4 shows the efficiency for some channels as a function of the χ^2 cut. A cut $\chi^2(rz) < 4$ is $\sim$100 % efficient. This step reduces the number of track candidates: there are in average 55 (r, z) Velo tracks in the direction of the spectrometer and from these, only 4.8 are matched to the L0 candidates.

These 4.8 tracks are converted into 3 dimensional (3D) Velo tracks adding the ϕ information of the Velo sensors. This corresponds to $\sim$10% of the total Velo 3D reconstruction. For consistency, these tracks are requested to match with the L0 candidates, using the same method described above, but the match is done in 3D instead of in the (r, z) plane. A $\chi^2(3D) < 4$ cut is applied.

In the next step, for each Velo track the minimum absolute IP to any primary vertex is computed. Figure 5 shows the efficiency for some channels as a function of the IP cut. A cut IP >0.1 mm is applied. This cut has a small loss in efficiency for some signal channels but it reduces the rate to 286 kHz and the number of candidates to 2.2. The IP cut is applied at this level to reduce the number of tracks to be reconstructed in the tracking stations.

In the next step, for every pair of matching 3D Velo track and a L0 candidate, a guided forward reconstruction is performed in the tracking stations. This guided reconstruction [11] uses the calorimeter position and the Velo direction to define a region of interest in the tracking stations. The data within that region is decoded. This represents 3% of the total decoding of the tracking stations. The pattern recognition algorithm uses only the hits inside the region of interest to search for a track and it takes $\sim$0.5 ms per track. After this step, the rate is 69 kHz. A good fraction of the matched candi-

	rate (kHz)	candidates	$B^0 \to h^+h^-$	$B_s^0 \to \Phi\Phi$	$B_s^0 \to D_s^\pm h^\mp$	$B^0 \to D^0 K^{*0}$
$E_{\rm T}$ >3.5 GeV	583	1.29	38.0	18.8	29.1	32.1
$\chi^2(rz)$ <4	555	4.81	37.9	18.3	28.6	31.9
Velo 3D	552	4.90	37.9	18.3	28.6	32.1
$\chi^2(3D)$ <4	511	3.26	37.6	17.8	27.9	31.2
IP >0.1 mm	286	2.17	36.0	15.8	27.1	28.6
Guided Forward	63	1.38	35.7	14.8	26.0	26.6
$P_{\rm T}$ >2.5 GeV	26	1.41	34.8	13.3	24.5	24.9

Table 3: Rate and number of candidates for mb events, and TOS efficiencies (in %) for some channels and for the different steps in the L0 confirmation sequence.

	per call (ms)	integrated (ms)
$E_{\rm T}$ >3.5 GeV	0.02	0.02
(r,z) Velo	0.85	0.87
PV	0.20	1.11
$\chi^2(rz)$ <5	0.10	1.21
3D Velo	0.40	1.58
$\chi^2(3D)$ <4	0.01	1.60
IP >0.1 mm	0.01	1.61
GuidedForward	0.85	2.04
$P_{\rm T}$ >2.5 GeV	0.01	2.04

Table 4: Time per execution (call) and total time to that step (integrated) for the different steps of the L0 confirmation sequence.

dates that pass the IP cut are fake combinations, that is, the 3D Velo track and the L0 candidate do not correspond to the same particle. When the guided forward reconstruction is applied on a fake pair, in most of the cases, no track is found in the tracking stations.

In order to obtain an output rate of ∼30 kHz, a cut on the $P_{\rm T}$ >2.5 GeV of the tracks is applied. This $P_{\rm T}$ cut somehow confirms the $E_{\rm T}$ cut of the L0 hadron candidate. Note that this cut has a small cost in efficiency (Fig. 6). Table 3 shows the rate and number of candidates for mb, and the TOS efficiency for some channels, for the different steps of the L0 confirmation. Note the the confirmation is 91% efficient for the L0 TOS $B^0 \to h^+h^-$ events and 71% for $B_s^0 \to \Phi\Phi$. One of the reasons of the loss of efficiency for the $B_s^0 \to \Phi\Phi$ is that the offline $B_s^0 \to \Phi\Phi$ seleccion cuts on the IP of the Φ instead of the IP of the individual hadrons. We have tried to replace the cut on $P_{\rm T}$ by a cut on $\frac{P_{\rm T}-E_{\rm T}}{\sigma_{E_{\rm T}}}$ without success due to the poor resolution of the $E_{\rm T}$ of the L0 hadron candidate.

Table 4 shows the time per execution (call) of each algorithm of the confirmation, and the integrated time (total time in the sequence down to that algorithm). Almost 1/2 of the time (1.11 ms) is used in the the reconstruction of the (r,z) Velo tracks and the primary vertices. The other major time consumption steps are the upgrade of the 4.8 (r,z) Velo tracks into 3D Velo tracks (0.44 ms) and the guided forward reconstruction for the 2.2, 3D Velo-L0 candidates pairs, that takes 0.43 ms more. Notice that the time spent in the selection algorithms is negligible compared to that used by the reconstruction algorithms.

4 Single hadron line

To reduce the output rate below 5 kHz, stronger cuts on IP or $P_{\rm T}$ are needed. A cut on $P_{\rm T} > 5$ GeV reduces the rate to 6.5 kHz, but it also reduces the signal efficiency. Table 5 shows the drops in TOS efficiency for some channels after the $P_{\rm T}$ cut. Notice that most of the efficiency of the hadron alley comes from the dihadron line that will be described in the next section. The single hadron gives robustness to the hadron trigger, as it only depends on one track. This line can be used at the start-up of the data taking when the luminosity and the L0 rates are going to be lower than in nominal conditions.

The studies at Ref. [12] have shown that 60% of the tracks that fired the single hadron line are "ghosts". Here, a track is said to be a ghost, if in any subdetector (Velo or tracking stations) the highest fraction of hits associated to a particle (according with the Monte Carlo) is smaller than 70%, or if the particles with the highest fraction of hits in any of the subdetectors are different. It has also been shown in [12] that 30% of the tracks that fire the single hadron line up to this level, come from the primary vertex, and pass the IP cut due to the "badly" measured track slopes. Approximately 60% of these tracks would not pass the IP

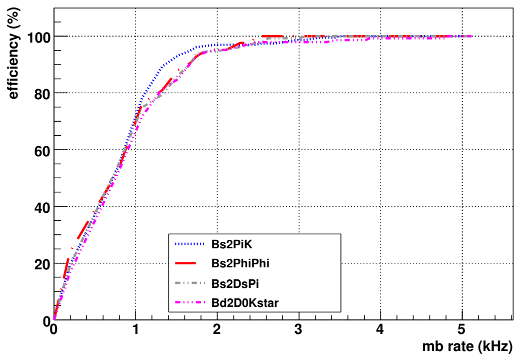

Figure 7: Efficiency vs rate as a function of the χ^2/ndf cut.

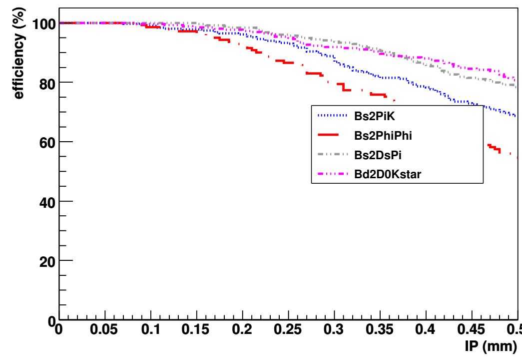

Figure 8: Efficiency vs the IP cut on the companion track.

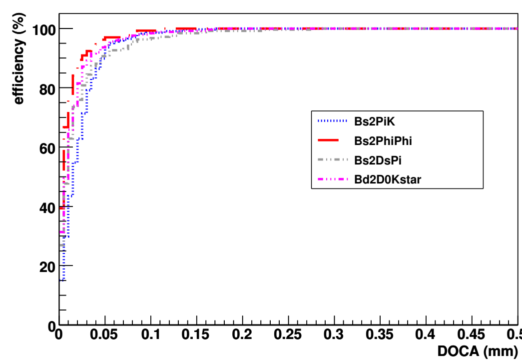

Figure 9: Efficiency vs the DOCA cut between the L0 confirmed and the companion tracks.

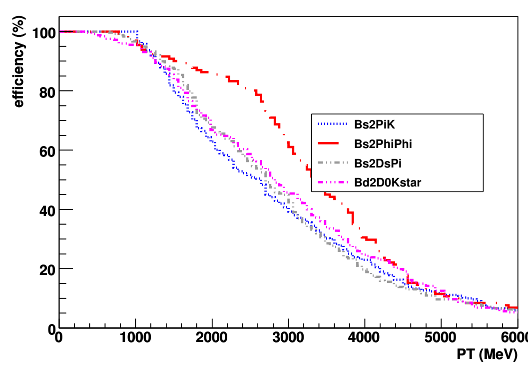

Figure 10: Efficiency vs the P_{T} cut on the companion track.

cut if the track was fitted with the offline Kalman fit.

In order to improve the quality of the tracks, a fast Kalman fit is applied to the tracks that pass the single hadron cuts. This fit is a simplified version of the offline Kalman fit. It uses a simplified detector geometry and operates a single pass (in the sense from the tracking stations to the Velo) and does not remove outlaier measurements from the fit. With this configuration, the fit takes in average 1 ms/track. The fit is applied to 1.4 tracks and at a rate of 6.5 kHz. Therefore, the total contribution to the time of the line is negligible, 0.15 ms. After the fit, the measurement of the track slope has improved for some tracks. Applying a IP cut (IP_{KF} >0.1 mm) the rate is reduced to 5.3 kHz.

Furthermore, the χ^2/ndf of the tracks is a good discriminant variable against ghosts. Fig. 7 shows the efficiency vs rate as a function of a χ^2/ndf cut. Requiring a χ^2/ndf <10, the output rate of the single line is 3.3 kHz and the number of tracks that fire the single hadron line is 1.3. This last step of the line reduces the mb output rate by factor 1/2. The studies of [12] have shown that still 40% of the tracks that fired the single hadron line are ghosts and that the fast Kalman fit has not the same performance as the offline Kalman fit. There are ongoing efforts to improve the fast Kalman fit and to find alternative methods to reduce the number of ghost tracks.

5 Di hadron line

In order to reduce the rate below 5 kHz, without imposing stronger cuts on the L0 confirmed track, the dihadron line requires that there is an extra track in the event, called companion track, forming a secondary vertex with the L0 confirmed track.

The search of the companion track starts with the reconstruction of all 3D Velo tracks. The rate at which the 3D Velo reconstruction is performed

	rate (kHz)	candidates	$B^0 \to h^+h^-$	$B_s^0 \to \Phi\Phi$	$B_s^0 \to D_s^\pm h^\mp$	$B^0 \to D^0 K^{*0}$
PT>5 GeV	6.5	1.41	23.6	4.2	13.3	14.5
IP_{KF} >0.1 mm	5.33	1.41	23.5	4.2	13.1	14.5
χ^2/ndf <10	3.34	1.30	23.4	4.2	13.1	14.2

Table 5: Rate and number of candidates for the mb, and TOS efficiencies (in %) for some channels, for the different steps of the single hadron line.

	rate (kHz)	candidates	$B^0 \to h^+h^-$	$B_s^0 \to \Phi\Phi$	$B_s^0 \to D_s^\pm h^\mp$	$B^0 \to D^0 K^{*0}$
P_{T} >2.5 GeV	26.0	1.41	34.8	13.3	24.5	24.9
Velo	26.0	56.1	34.8	13.3	24.5	24.9
IP_2 >0.1 mm	26.0	30.4	34.8	13.3	24.5	24.9
DOCA<0.2 mm	25.4	14.6	34.5	13.2	24.3	24.9
Δz >1.5 mm	22.8	6.02	34.1	13.1	23.9	24.7
Forward	19.8	4.53	33.1	13.1	23.8	24.7
P_{T2} >1 GeV	6.5	2.57	33.1	12.7	23.0	23.6
Pointing<0.4	5.3	2.58	33.1	12.6	23.0	23.6
IP_{KF} >0.1 mm	4.2	2.76	32.9	12.1	22.7	23.4
χ^2/ndf <10	2.7	2.03	32.2	11.9	22.5	23.2

Table 6: Rate and number of candidates for the mb, and TOS efficiencies (in %) for some channels, for the different steps of the dihadron line.

is 26 kHz [1]. The companion tracks are required to have an IP larger than 0.1 mm (IP_2 >0.1 mm). This cut is almost 100% efficient (see Fig. 8). In the next step, a secondary vertex is created if the distance of closest approach, DOCA, between a L0 confirmed track and a companion track, is lower than 0.2 mm (DOCA<0.2 mm). The closest point between the two tracks is taken as the vertex position. Figure 9 shows the efficiency as a function of the cut on DOCA. This cut is 100 % efficient even for the $B_s^0 \to D_s^\pm h^\mp$ channel.

In the next step, these secondary vertices are required to have a minimum distance in z (Δz) with respect to its closest primary vertex. Figure 11 shows the efficiency vs the Δz distance cut. A cut Δz >1.5 mm is applied. This cut does not reduce the rate, but it reduces the number of vertex candidates to 6. In the next step, the companion tracks are reconstructed in the tracking stations using the forward reconstruction [13]. There are ~ 4.6 tracks to be reconstructed forward at a rate of 23 kHz. Only vertices with a companion track with P_{T2} >1 GeV are kept. Figure 10 shows that this cut has a small loss in efficiency for multi-body decays while it reduces the rate to 6.4 kHz.

[1]The possibility of applying the Kalman Filter to the confirmed tracks before doing the 3D Velo reconstruction is currently under investigation

Finally, the sum of the momenta of the two tracks in the secondary vertex is required to point to the primary one. The following "pointing" quantity is computed: $\frac{\mathbf{p}\ \mathbf{u(SV-PV)}}{P_{T1}+P_{T2}}$; where $\mathbf{p}$ es the sum of the momenta of the two particles; $\mathbf{u}(\mathbf{SV}-\mathbf{PV})$ is the unitary vector between the position of the secondary vertex ($\mathbf{SV}$) and the primary one ($\mathbf{PV}$); and $P_{\mathrm{T1}}+P_{\mathrm{T2}}$ are the sum of the transverse momentum of the tracks. This variable uses the constraint that in the plane perpendicular to the flight B direction, the sum of the momenta of the B daughters should be close zero. Figure 12 shows the efficiency vs the pointing cut. A cut at 0.4 is applied. Table 6 shows the rate and number of candidates for the mb, and the TOS efficiency for some channels, for the different steps of the dihadron line. At this stage, the output of the dihadron line is 5.3 kHz, and the efficiency for most of the channels is very similar to the one obtained after the L0 confirmation part.

As in the single hadron line, the dihadron line has a final part, where the tracks are fitted using the fast Kalman fit. A cut on IP_{KF} >0.1 mm and in χ^2/ndf <10 are applied in order to eliminate badly reconstructed and ghost tracks. Table 6 shows that this step reduces the rate by almost 1/2 to a final rate of 2.8 kHz. The number of vertices that fired the dihadron lines is 2. The extra

	$B^0 \to h^+h^-$	$B_s^0 \to \Phi\Phi$	$B_s^0 \to D_s^{\pm}h^{\mp}$	$B^0 \to D^0K^{*0}$
total eff (%)	33	12.5	23.3	23.9
TOS eff (%)	32.2	11.9	22.5	23.2

Table 7: total and TOS efficiency of the dihadron line for some channels.

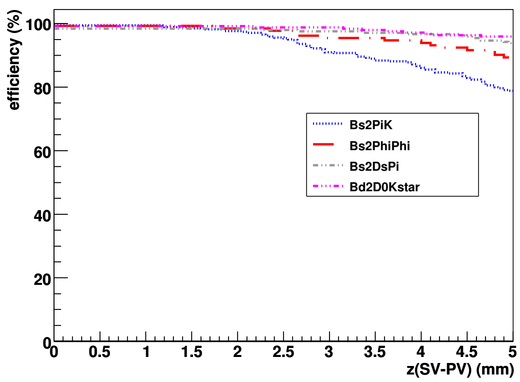

Figure 11: Efficiency vs the cut on Δ_z, the distance in z between the secondary and primary vertices.

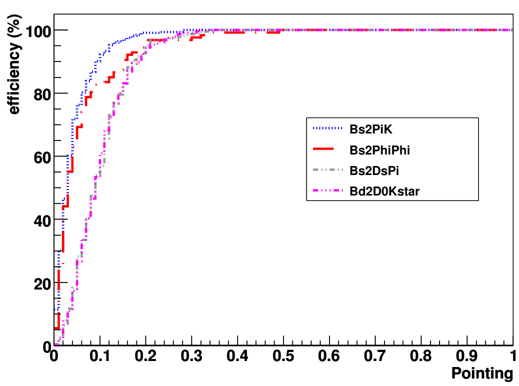

Figure 12: Efficiency vs the pointing cut.

time that the dihadron line takes with respect to the single line is 0.35 ms at the input rate of 580 kHz. The algorithms that dominate the time consumption are the 3D Velo and the forward reconstruction of the companion tracks.

Table 7 shows the dihadron total and TOS efficiency for some channels. Note that almost all the efficiency of the line comes from TOS events. This is a consequence of the L0 confirmation. A selected B decay event, that is not TOS at L0, is likely rejected either by the L0 confirmation or the IP cut.

6 Alternative configurations

The default hadron alley configuration, described in the previous sections, has a set of cuts on IP and P_{T} of the L0 confirmed and companion tracks, such that the output rate is reduced to 30 kHz after the L0 confirmation part and below 5 kHz after the dihadron decision. Nevertheless, there is a loss in TOS efficiency for some multi-body decays such as $B_s^0 \to \Phi\Phi$ and $B^0 \to D^0K^{*0}$. In this section, some alternative configurations of the L0 and hadron alley are presented, which will increase the efficiency at the cost of using extra CPU time and producing a higher output rate.

6.1 Reduced IP and PT cuts

In this configuration, the IP and P_{T} cuts on the L0 confirmed and companion tracks are softened to gain efficiency. In order to get ~98% efficiency in each step, the following cuts are set: IP >0.06 mm (Fig. 5) and P_{T} >1.5 GeV for the L0 confirmed track and $P_{\mathrm{T}2}$ >0.8 GeV for the companion one (Figs. 6 and 10). Table 8 shows the rate and number of candidates for mb and the TOS efficiencies for some channels, for the different steps of the dihadron line. The rate of the L0 confirmation part increases to 94 kHz, a factor 3, and the final rate is 14.5 kHz, to be compared with 2.7 kHz in the default configuration. The last step of the line, using the track fitted by the fast Kalman filter, reduces the rate by a factor ~1/2. This configuration is 83 % efficient on L0 TOS $B_s^0 \to \Phi\Phi$ events and 86 % for $B^0 \to D^0K^{*0}$, but produces ~10 kHz more of output rate.

6.2 Removing the GEC

The GEC reduce the efficiency depending on the channel. Without GEC, to keep the hadron rate at 600 kHz, the cut on E_{T} at L0 must be 4 GeV (see Fig. 13). Fig. 14 shows the L0 TOS efficiency for some channels vs the E_{T} cut. Table 9 shows the L0 TOS efficiencies for the L0 hadron with and without GEC. Without GEC, the $B^0 \to h^+h^-$ channel gains in efficiency while the gain is smaller for $B_s^0 \to \Phi\Phi$. The L0 confirmation strategy is based

	rate (kHz)	candidates	$B^0 \to h^+h^-$	$B_s^0 \to \Phi\Phi$	$B_s^0 \to D_s^{\pm}h^{\mp}$	$B^0 \to D^0K^{*0}$
IP >60 μm	357	2.51	37.5	17.3	27.9	30.2
GuidedForward	128	1.42	37.2	16.6	27.2	29.3
$P_{\rm T}$ >1.5 GeV	94	1.39	37.2	16.5	27.0	29.0
3D Velo	94	53.4	37.2	16.5	27.0	29.0
IP_2 >60 μm	94	38.0	37.2	16.5	27.0	29.0
DOCA<0.2 mm	94	24.9	37.1	16.5	26.8	29.0
Δz >1.5 mm	86	7.03	36.6	16.2	26.4	28.8
Forward	78	5.30	35.5	16.2	26.3	28.8
$P_{\rm T2}$ >0.8 GeV	33	2.31	35.5	16.0	26.0	28.1
Pointing<0.4	28	2.22	35.5	16.0	26.0	28.1
IP_{KF} >60 μm	18.5	2.29	35.4	15.7	25.9	27.8
χ^2/ndf <10	14.5	1.91	34.7	15.6	25.6	27.7

Table 8: Rate and number of candidates for the mb, and TOS efficiencies (in %) for some channels, for the different steps of the dihadron line with lower cuts on IP and $P_{\rm T}$ of the L0 confirmed and companion tracks.

on the reconstruction of the tracks associated to the L0 candidates and this number is still small (1.3) after removing the GEC, as can be seen in Fig. 15. Table 10 shows the rate and number of candidates for the mb, and signal TOS efficiencies, for some steps of the dihadron line where events are not vetoed at L0 by GEC. Note that the output rate of the L0 confirmation part has increased to 39 kHz, while the final output rate has increased to 3.5 ± 0.5 kHz. There is a gain in efficiency for all the channels.

6.3 Soft dihadron line

The following configuration, called "soft dihadron line", improves the efficiency lost in the confirmation of the L0 candidates that are non TOS at L0. Here, the L0 confirmation uses all L0 events and starts from any L0 hadron cluster with a $E_{\rm T}$ above a lower threshold than the one set to trigger the L0 hadron. In the L0 non TOS events, a L0 hadron cluster produced by the B daughters could exist, but its $E_{\rm T}$ value is below the L0 hadron threshold; therefore, starting the alley from candidates with a lower $E_{\rm T}$ threshold, some of these L0 hadron clusters will be used as seeds. Fig. 16 shows the input rate vs the $E_{\rm T}$ threshold. At $E_{\rm T}$ >2.5 GeV the input rate of the hadron alley is now 730 kHz. Fig. 17 shows the TOS efficiency vs the $E_{\rm T}$ threshold. The knee in the curve corresponds to the actual cut on the L0 hadron trigger at $E_{\rm T}$ >3.5 GeV. Table 9 shows the L0 TOS efficiency for the default configuration and with a $E_{\rm T}$ cut of $E_{\rm T}$ >2.5 GeV. In this case, the efficiency for the $B_s^0 \to \Phi\Phi$ channel increases from 19% in the default configuration to 26%. The number of L0 candidates has also increased (see Fig 18) to 1.85. The $P_{\rm T}$ cut of the L0 confirmed has been reduced accordingly to 1.5 GeV. Table 11 shows the rate and number of candidates for mb and signal TOS efficiency, for some steps in the dihadron alley for the soft configuration with the initial threshold of $E_{\rm T}$ >2.5 GeV. The final $B_s^0 \to \Phi\Phi$ efficiency is 18.4%, while the output rate has doubled: at the intermediate step of the L0 confirmation is 66 kHz and the final rate is ∼6 kHz. The CPU time consumed by this line is 66% more than the one used by the dihadron line.

6.4 Comparison

In order to compare the performance of the different configurations, the following Figure of Merit (FoM) has been computed: the ratio between the increase of efficiency and the increase of rate with respect the default configuration. The FoM measures the increase of efficiency per extra kHz of output rate. Table 12 shows the FoM values for the different channels and configurations. The best performance corresponds to the configuration without GEC. The gain is different for different channels; in particular it is large for $B^0 \to h^+h^-$. Also the output rate of this configuration at the L0 confirmation and final part are only ∼30% more than the default configuration. The second best configuration is the soft dihadron alley. In this case the gain is similar for all the channels, including $B_s^0 \to \Phi\Phi$. These two configurations are complementary, that is, signal events gained removing the GEC are different from those ones obtained in the soft dihadron alley. Therefore the combination of

	$B^0 \to h^+h^-$	$B_s^0 \to \Phi\Phi$	$B_s^0 \to D_s^\pm h^\mp$	$B^0 \to D^0 K^{*0}$
default ($E_{\rm T}$ >3.5 GeV)	38.0	18.8	29.1	32.1
without GEC ($E_{\rm T}$ >4 GeV)	48.3	22.0	34.9	38.4
soft ($E_{\rm T}$ >2.5 GeV)	44.5	25.8	36.6	38.7

Table 9: L0 TOS efficiency (in %) for the default, without GEC and soft dihadron line, alley configurations.

	rate (kHz)	candidates	$B^0 \to h^+h^-$	$B_s^0 \to \Phi\Phi$	$B_s^0 \to D_s^\pm h^\mp$	$B^0 \to D^0 K^{*0}$
$E_{\rm T}$ >4 GeV	596	1.30	48.3	22.0	34.9	38.4
$P_{\rm T}$ >2.5 GeV	39	1.40	44.3	16.5	30.1	30.3
Pointing<0.4	7.9	1.87	41.2	15.3	28.3	28.4
χ^2/ndf <10	3.5 ± 0.5	1.57	40.2	14.6	27.6	27.9

Table 10: Rate and number of candidates candidates for the mb, and TOS efficiency (in %) for some channels, for some steps in the dihadron alley without applying GEC at L0.

	rate (kHz)	candidates	$B^0 \to h^+h^-$	$B_s^0 \to \Phi\Phi$	$B_s^0 \to D_s^\pm h^\mp$	$B^0 \to D^0 K^{*0}$
$E_{\rm T}$ >2.5 GeV	727	1.85	44.5	25.8	36.6	38.7
$P_{\rm T}$ >1.5 GeV	66	1.43	42.5	20.6	33.1	32.6
Pointing<0.4	11.20	2.39	40.2	19.1	30.9	30.7
χ^2/ndf <10.0	6.0 ± 0.5	2.08	39.1	18.4	30.5	30.2

Table 11: Rate (kHz) and number of candidates for the mb, and TOS efficiency (in %) for some channels and for some steps in the soft dihadron line.

	$B^0 \to h^+h^-$	$B_s^0 \to \Phi\Phi$	$B_s^0 \to D_s^\pm h^\mp$	$B^0 \to D^0 K^{*0}$
reduced IP,$P_{\rm T}$ cuts	0.2	0.3	0.25	0.4
without GEC at L0	10	3.3	6.3	6
soft dihadron	3	2.8	3.4	3

Table 12: The ratio of the increase in efficiency (in %) and the increase in rate (in kHz), with respect the default dihadron line, for some channels and for different configurations: reducing IP and $P_{\rm T}$ cuts, without GEC at L0, and in the soft dihadron line configuration.

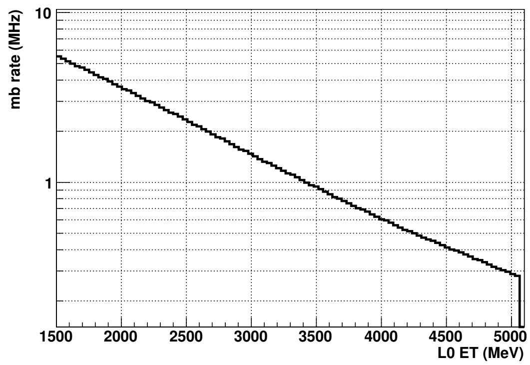

Figure 13: Rate vs the E_{T} cut without GEC at L0.

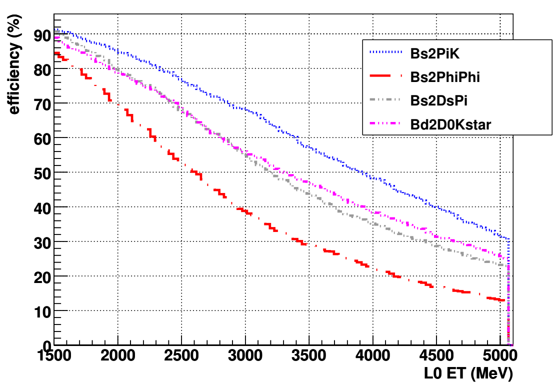

Figure 14: L0 TOS efficiency (in %) vs the E_{T} cut, without GEC at L0.

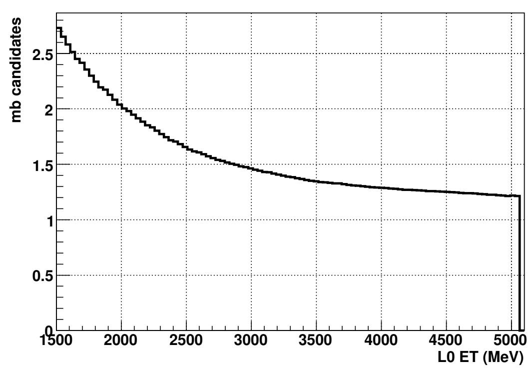

Figure 15: Number of L0 candidates above a given E_{T} cut for mb events, without GEC at L0.

both configurations should have higher efficiency.

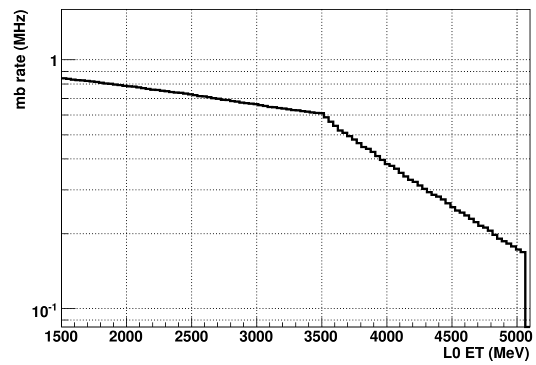

Figure 16: Rate (in MHz) vs the E_{T} cut for mb events, for the soft dihadron line.

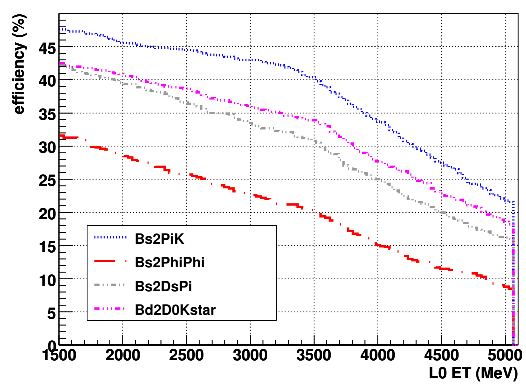

Figure 17: TOS L0 efficiency (in %) vs the E_{T} cut, for the soft dihadron line.

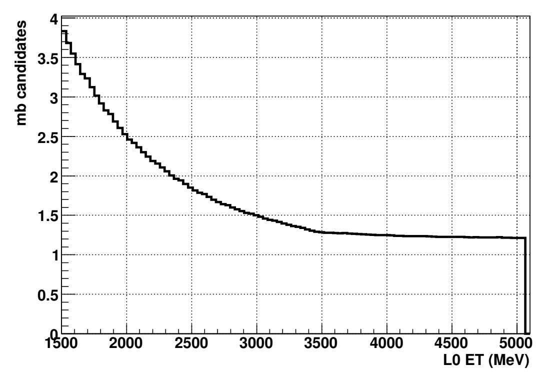

Figure 18: Number of L0 candidates above a given E_{T} cut for mb events, for the soft dihadron line.

7 Conclusion

The hadron alley based on the confirmation strategy has been described in the note. The alley can reduce the rate to 5 kHz, while keeping the TOS efficiency high for most of the signal channels: 84% for $B^0 \to h^+h^-$ and 78% for $B_s^0 \to D_s^{\pm}h^{\mp}$. With the L0 confirmation strategy only few tracks are reconstructed per event. This strategy is quite efficient for L0 TOS events but fails in L0 non TOS events. Three alternative configurations have been presented: reducing the IP and P_{T} cut of the confirmed and companion tracks; removing the GEC at L0; and the soft dihadron line, that starts the L0 confirmation from a hadron cluster with lower E_{T} threshold that the one used in the L0 hadron trigger. The hadron alley without GEC has a particulary good performance, due to the fact that there are few L0 hadron candidates to start with, even without GEC.

Acknowledgments

The authors thank H. Dijkstra and F. Teubert for their comments and ideas that have helped to shape the hadron alley; and H. Ruiz, for his comments and corrections to this note.

References

[1] The LHCb collaboration, *The LHCb Detector at LHC* Journal of Instrumentation (JINST), 2008 JINST 3 S08005

[2] S. Amato, A. Satta, B. Souza de Paula, L. de Paula, *Hlt1 Muon Alley description*, CERN-LHCb-2008-058

[3] A. Pérez-Calero, H. Ruiz, *The muon+track Alley of the LHCb High Level Trigger*, CERN-LHCb-2008-075

[4] B. Souza de Paula, *Studies on Systematics Effects of the Trigger on Flavour Tagging at the Generator Level*, CERN-LHCb-2006-046

[5] J.A. Hernando, E. Lopez Asamar, D. Martinez Santos, H. Ruiz, F. Teubert *Measurement of trigger efficiencies and biases*, CERN-LHCb-2008-073

[6] The LHCb collaboration, *LCHCb Trigger System, Technical Design Report*, CERN LHCC 2003-031, LHCb TDR 10

[7] J. Albrecht *Fast T-Station Seeding for HLT1*, CERN-LHCb-2009-012

[8] J. Albrecht *L0 Confirmation with fast, Tsa based tracking in the T-stations*, CERN-LHCb-2007-118

[9] M. Krasowski, M. Kucharczyk, W. Männer, G. Polok, M. Witek, *Primary vertex reconstruction*, CERN-LHCb-2007-011

[10] N. Zwahlen, *HLT Hadronic L0 Confirmation*, LPHE Note 2006-14, CERN-LHCb-2006-040

[11] J. Albrecht *T-hits in a search window defined by a velo confirmed hadronic L0*, TRec presentation, 14th March 2008

[12] X. Cid, *Use of the Kalman Filter in the Hadron alley*, TRec presentation, 15th December 2008, (LHCb note in preparation)

[13] O. Callot, S. Hansmann-Menzemer, *The Forward Tracking: Algorithm and Performance Studies*, CERN-LHCb-2007-015